

## Studies of oxide glass structure using laser ionization time of flight mass spectrometry

This article has been downloaded from IOPscience. Please scroll down to see the full text article.

2003 J. Phys.: Condens. Matter 15 S2323

(<http://iopscience.iop.org/0953-8984/15/31/308>)

View [the table of contents for this issue](#), or go to the [journal homepage](#) for more

Download details:

IP Address: 171.66.16.125

The article was downloaded on 19/05/2010 at 14:58

Please note that [terms and conditions apply](#).

# Studies of oxide glass structure using laser ionization time of flight mass spectrometry

Mario Affatigato<sup>1</sup>, Steve Feller, Allison K Schue, Sarah Blair,  
Dale Stentz, Garret B Smith, Dan Liss, Matt J Kelley, Cole Goater and  
Raghuvir Leelesagar

Physics Department, Coe College, 1220 First Avenue NE, Cedar Rapids, IA 52402, USA

E-mail: maffatig@coe.edu

Received 21 February 2003

Published 23 July 2003

Online at [stacks.iop.org/JPhysCM/15/S2323](http://stacks.iop.org/JPhysCM/15/S2323)

## Abstract

We report on our work on determining the structure of oxide glasses using laser ionization time of flight mass spectrometry. This technique is especially suitable for investigation of the intermediate-range order in glasses, where it can measure the presence and relative abundance of mesounits composed of 7–20 or more atoms. After introducing the experimental aspects and caveats of this new spectroscopy, we discuss the application of the instrument to a variety of heavy-metal oxide glass families. We separate our networks into those that have superstructural networks and those that show highly fragmented ones, including our studies of lead and bismuth borates, lead silicates, lead vanadates, and bismuth gallates. We also analyse our spectra for evidence of mixing in lead borosilicates, and to clarify the sharing of cations in sodium-doped lead borosilicates.

(Some figures in this article are in colour only in the electronic version)

## 1. Introduction

The past few decades have brought great advances in the understanding of the structure of oxide glasses. As new structural characterization techniques have come into existence, the knowledge of the network arrangement has grown dramatically. In particular, optical techniques such as FTIR and Raman [1], and other approaches including neutron and x-ray scattering, and solid-state nuclear magnetic resonance (NMR) have been among the most productive. They have elucidated many questions on the structural details of oxide and non-oxide glasses. Amongst their more important contributions is a clear understanding of the arrangement of atoms at the nanoscale, which establishes the short-range order of the glass. We refer to these groupings of 4–6 atoms as *nanounits*.

<sup>1</sup> Author to whom any correspondence should be addressed.

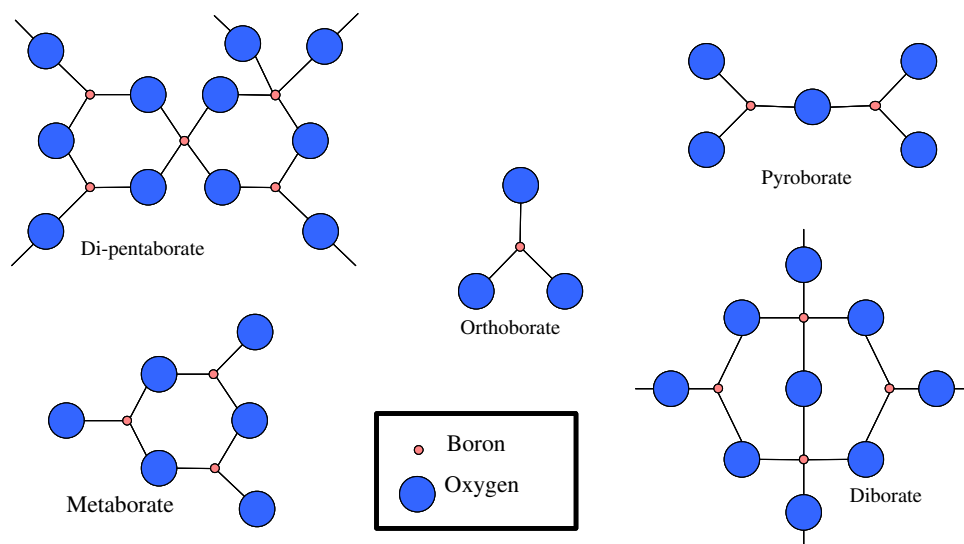


**Figure 1.** Some borate nanounits and mesounits derived from alkali borate crystals.

Even after these great advances, important structural questions remain. The most important of these refers to the presence or absence of superstructural units in the glass network. These *mesounits* establish an intermediate- or medium-range order in the oxide structure, affecting a variety of the properties of the glass, and they are typically constituted by 7–20 or more atoms. Preliminary information on the possible arrangement of these mesounits can be derived from the study of crystal structures isocompositional with the glasses. Figure 1 shows some [2] of these groupings obtained from alkali borate crystals. Typically, the infrared or Raman signatures of the mesounits can then be measured from the crystals, and the glasses can be checked for the presence or absence of these signatures. This signature is not, however, quantifiable without the hard-to-get oscillator strengths of the individual units.

Recent advances in neutron [3] and x-ray scattering [4] as well as NMR [5–8] have allowed for further scrutiny of the intermediate-range order. Inelastic neutron scattering provides a better look [9, 10] at the vibrational density of states than either infrared or Raman spectroscopy, and it can attain quantitative results.

All of the techniques mentioned above have the significant advantage of being well tested over a period of decades. They all suffer, however, from some disadvantages. Infrared and Raman spectroscopies do not easily yield quantitative information; neutron and x-ray scattering often require expensive isotope enrichment and large-scale instrumental facilities; and solid-state NMR can be difficult to interpret. The current article is a summary of our work, and of the ways in which it can complement these existing techniques.

Laser-induced ionization time of flight mass spectrometry (LITOF-MS) is a technique new to the field of glass science. The instrument works by gently desorbing fragments of the glass network using a low-power laser, avoiding any surface damage. The mass of the units is then determined with extremely high (sub-isotopic) accuracy using a time of flight mass spectrometer. Isotopic simulation then yields the exact chemical composition of the fragments, which can then be used to derive structural insights and attempt a reconstruction of the sample structure. The technique has several advantages, including ease of interpretation, relatively low cost, no need for special sample preparation, and applicability to all glass systems that absorb at the laser wavelength.

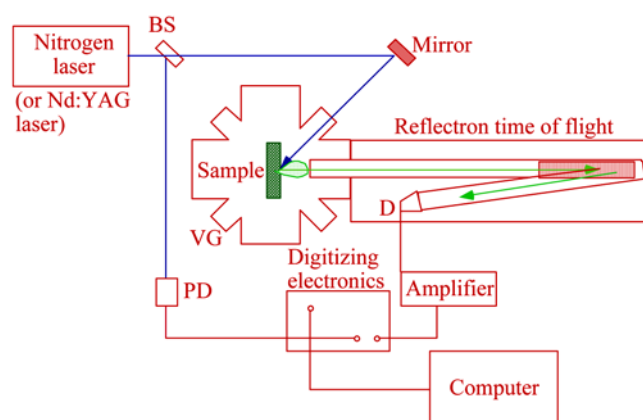


**Figure 2.** An instrumental diagram of the laser ionization time of flight mass spectrometer.

In this paper we will present a review of our work on the determination of glass structure using LITOF-MS, and we report on our studies of heavy-metal oxide systems, including lead borates, lead silicates, lead borosilicates, lead vanadates, sodium-doped lead borosilicates, and bismuth gallates.

## 2. Experimental procedure

### 2.1. The set-up of the LITOF-MS instrument

Figure 2 illustrates the instrumental set-up of the spectrometer. A low-power nitrogen laser (337.1 nm,  $<100 \mu\text{J}/\text{pulse}$ , 10 Hz) is used to irradiate the sample which is inside a vacuum chamber at  $10^{-7}$  Torr. The laser pulses are 4 ns long, yielding a peak power of only 25 kW. The fragments that are thus desorbed are extracted from the source region using a time-delayed electric field pulse, and then fly down a drift tube. An ion mirror then reverses their direction, attaining an even better mass resolution, and the ionic fragments then arrive at a microchannel plate detector. The instrument can only measure positive or negative ions separately, and cannot detect neutral atoms in its present configuration.

Each time the laser fires, a signal is sent to the data acquisition board, which then times the arrival of all the fragments. The instrument must have been previously calibrated for mass arrival times using known standards, such as NaCl, KCl, and, if higher masses are needed, PbO. The computer can then display a mass spectrum, in which the mass/unit charge (in amu/e) is on the  $x$ -axis, and the signal intensity, proportional to the number of ions of that particular mass, is shown on the  $y$ -axis. The charge on a particular group cannot be determined from its location on the mass spectrum, but is easily measured from the separation of the individual isotopic components.

The resolution of the instrument is sub-isotopic, with a typical value  $M/\Delta M = 1500$ . Taking into account peak width and shot-to-shot and sample-to-sample variability, we estimate the net mass error to be 0.4 amu. We also note that each spectrum reported here is an average of 200 individual mass spectra, each originated by a laser pulse.

### 2.2. Optical absorption and laser damage

One of the key requirements of the technique is that the sample must have a reasonably strong absorption at the laser wavelength, currently 337 nm. This is normally not a major difficulty,

as many glasses absorb at 337 nm due to impurities, defects, dopants, or a major constituent. Because our samples are made from high-purity starting chemicals, we chose to use lead or bismuth as a major constituent, given the strong absorption of these glasses arising from the metal cations.

Although the laser power is low, damage is always a concern. This technique can only be used for structural characterization if each laser shot does not alter the surface significantly. Otherwise the next laser shot might see (and desorb) a chemically different glass after every laser pulse. To check for this we obtained scanning electron micrographs (SEM) for multiple glass samples after several thousand shots at full power (no attenuation). The surfaces are unscathed after this treatment, virtually unrecognizable from the unirradiated control samples. Figure 3 shows a comparison of two such sample surfaces, and then shows the difference from a surface exposed to irradiation from a Nd:YAG higher-power laser.

Mechanisms for damage and desorption are quite complex [11] and beyond the scope of this paper. Nevertheless, we note that the optical absorption of lead- and bismuth-containing samples has been attributed [12–14], when at low concentrations, to the  $^1S_0 \rightarrow ^3P_1$  transition of the lead and the bismuth metal cations. It is therefore logical to assume that the desorption mechanism may involve the disruption of the network through the fracture of Pb–O and Bi–O bonds upon light absorption by outer electrons. The absorption of the laser energy by the metal cations should also help to preserve the important anionic network, and suppress the possibility that the mesounits will fragment.

### 2.3. Spectral analysis

Figure 4(a) displays a typical negative-ion time of flight spectrum from a lead silicate glass. The resolution of the data is high enough that mass multiplets appear condensed in the figure, and thus figure 4(b) is a zoom of the  $PbSiO_3$  multiplet. Each individual peak corresponds to a variation of the  $PbSiO_3$  group, each composed of a different combination of isotopes of lead, silicon, and oxygen. It is this signature pattern that allows for the clear, unambiguous identification of the elements that compose each mass grouping. IsoPro<sup>®</sup> is modelling software that simulates what the spectral feature ought to look like given a guess of the atomic components and the natural abundance of their isotopes. Figure 4(b) also shows the result of one such simulation for the  $PbSiO_3$  group. The clear match between the simulation and the data, down to smallest features, is unambiguous evidence that this mass multiplet is indeed  $PbSiO_3$ . Further confirmation can be obtained by using isotopically enriched starting compounds and comparing the relative mass shifts in the individual peaks in the spectra.

For clarity, we note that by convention we will refer to the largest mass peak in the multiplet when discussing the individual units, which are often made up of several peaks. Also, all of the units reported herein have a charge of  $\pm 1$ , regardless of the valences of the ions that constitute them. This is quite common in laser desorption.

### 2.4. Sample preparation and limitations of the technique

The sample preparation for LITOF-MS is quite simple. A glass is prepared from high-purity starting compounds to prevent contamination. A flake, chunk, or powder sample is taken and mounted onto a stainless steel tip that is then inserted into the spectrometer. The vacuum pressure is lowered to the required  $5 \times 10^{-7}$  Torr, and the sample is then run. Our best results have been obtained from powders, most probably because of the abundance of edges and corners in the grains, which may aid laser desorption.

Finally, we would like to point out some of the limitations of the LITOF-MS technique, some of which may be resolved in the future:

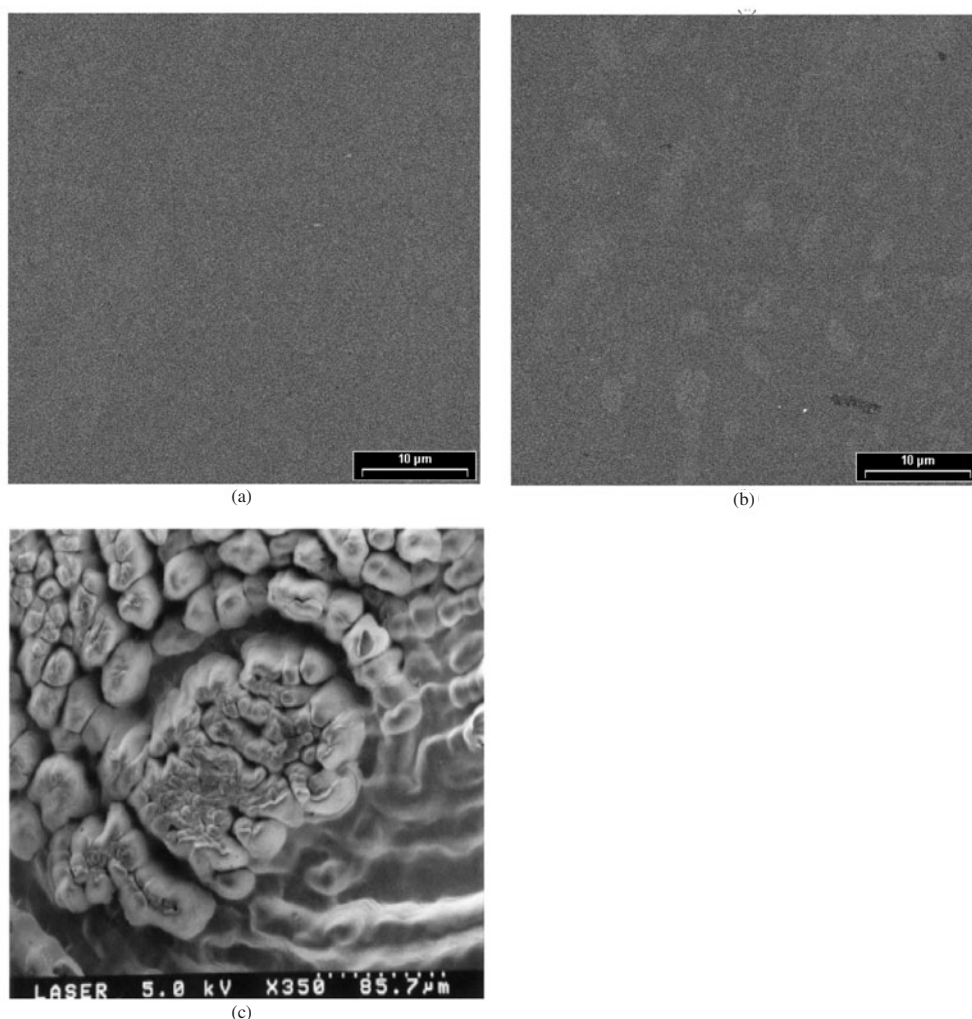


**Figure 3.** (a) The unirradiated region of a lead borate glass ( $2\text{PbO}\cdot\text{B}_2\text{O}_3$ ) and (b) the same glass after an irradiation of 4000 nitrogen laser shots at  $100\ \mu\text{J}/\text{pulse}$ . The slightly discoloured spots also appeared in other unirradiated areas, and thus are not caused by the laser light. Micrograph (c) shows the substantially different damage after 600 Nd:YAG laser shots (266 nm; 50 mJ).

- (a) The sample must absorb strongly at the laser wavelength, which in our case is 337.1 nm. This may be done intrinsically (preferred) or by doping with chromophores.
- (b) The sample must be free of contaminants that could shift the mass peaks in unknown ways, making analysis impossible.
- (c) The technique is incapable of describing the geometry (conformation) of the desorbed mass fragments.
- (d) The technique cannot detect fragments that are desorbed as neutral species. This is a limitation that can be overcome using a secondary-ionization laser beam.
- (e) The spectrometer we use cannot detect masses above 5000 amu, limiting its use when large organics or biomolecules may be involved.

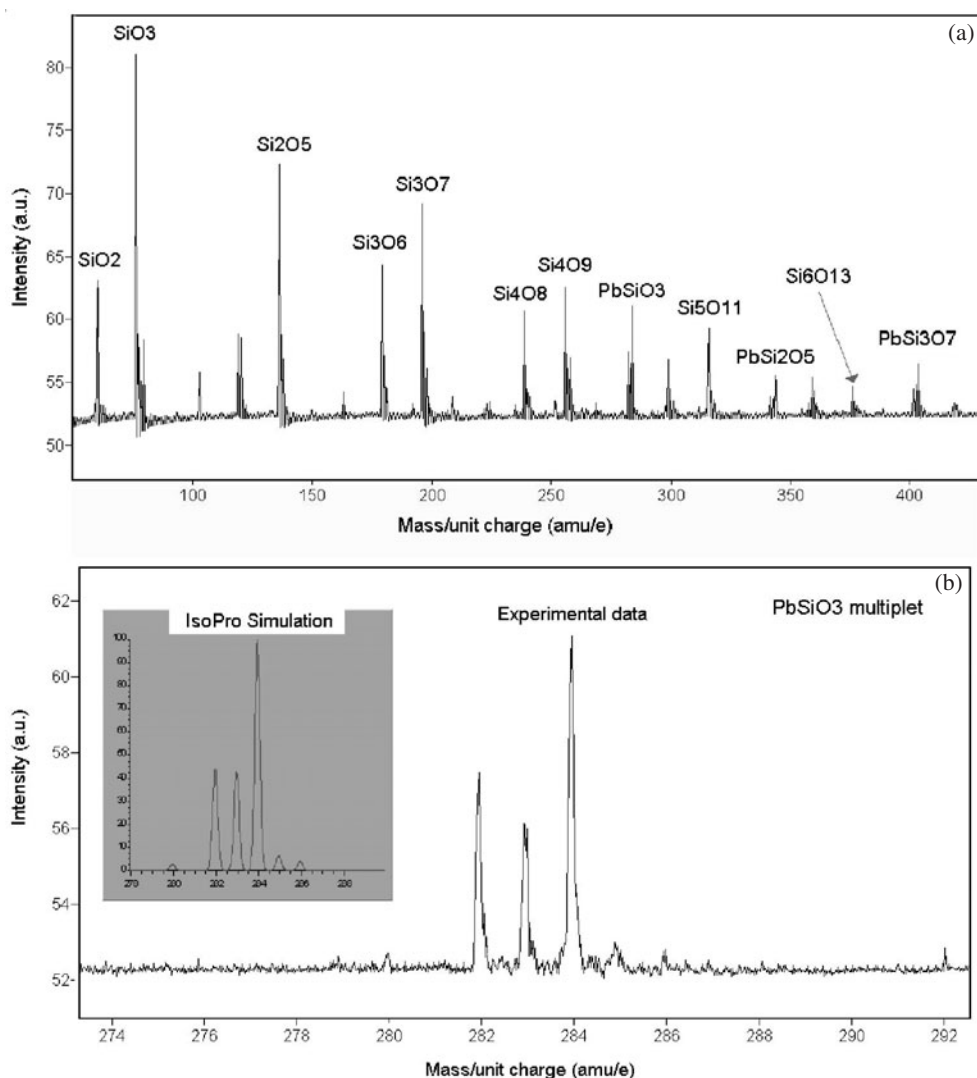


**Figure 4.** (a) A sample negative-ion mass spectrum from a 2PbO·SiO<sub>2</sub> glass; (b) shows a comparison between the experimental PbSiO<sub>3</sub> multiplet and the IsoPro<sup>®</sup> simulation.

None of the above limitations are especially severe, but they require further work to reduce their number. Work is ongoing in our laboratory to resolve some of these issues.

### 3. Results and discussion

In this section we will summarize what we consider to be some of the greatest contributions of the LITOF-MS technique to the study of glass structure to date. We note that the list is not meant to be comprehensive, but rather representative of the capabilities of the instrument.

#### 3.1. Binary glass systems

In the binary oxide glass systems we have studied the bismuth borates, the lead borates [15], bismuth gallates, lead vanadates, and lead silicates. All of these systems were studied over



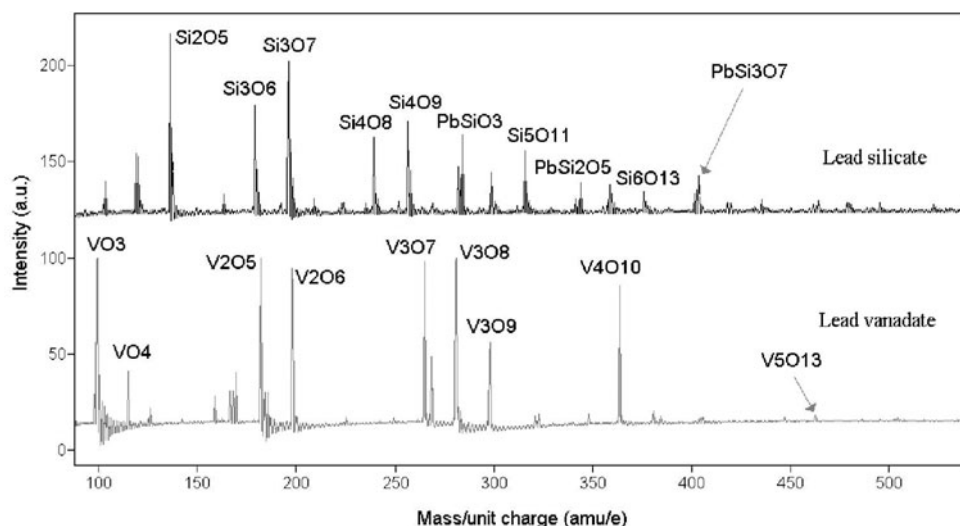
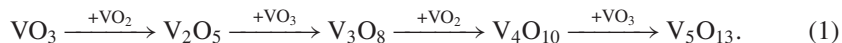


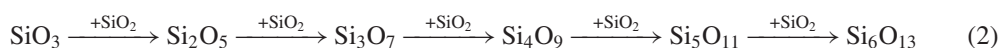
**Figure 5.** Comparison of lead silicate (top:  $2\text{PbO}\cdot\text{SiO}_2$ ) and lead vanadate (bottom:  $1.5\text{PbO}\cdot\text{V}_2\text{O}_5$ ) negative-ion mass spectra.

fairly wide compositional ranges, though a minimum lead content was necessary to ensure the strong optical absorption of each sample. In general, the results pointed to two kinds of network: highly fragmentary and superstructural.

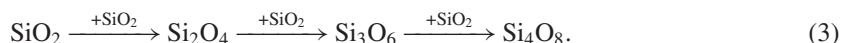
**3.1.1. Fragmented networks.** The highly fragmentary networks include the lead silicates and the lead vanadates. They are characterized by mass spectra rich in mass peaks which can be reproduced by repeatedly adding one or two small basic units. The lead vanadate and lead silicate spectra are shown for comparison in figure 5. Most of the peaks in this negative spectrum can be constructed by adding  $\text{VO}_2$ ,  $\text{VO}_3$ , or  $\text{SiO}_2$  units. Thus, for the most intense mass peaks in the lead vanadates,



For the negative lead silicates, the construction is similar, yielding



and



Other units in the negative spectra can be attained by adding a lead cation to the existing vanadate (or silicate) anionic units, as in the case of  $\text{PbSiO}_3$ ,  $\text{PbSi}_2\text{O}_5$ , and  $\text{PbSi}_3\text{O}_7$ . The conclusion drawn from these systems is that their networks are made up of basic units. We note that this does not mean that larger units are not present (such as four-membered silica rings), but rather that these larger units do not appear to be more stable than the sum of the individual units. Other units in the spectra indicate that lead attaches to some of the basic silicate groups, never forming more complex molecular structures. This is reinforced by the observation of  $\text{Pb}^+$  and  $\text{Pb}_2^+$  ions in the positive spectra. This behaviour begins to change at higher lead contents, when lead oxide ( $\text{Pb}_2\text{O}^+$ ,  $\text{Pb}_3\text{O}_2^+$ ) groups begin to grow at the expense of the metallic lead peaks. Thus, upon desorption, the fragments leave the sample in simple molecular forms,



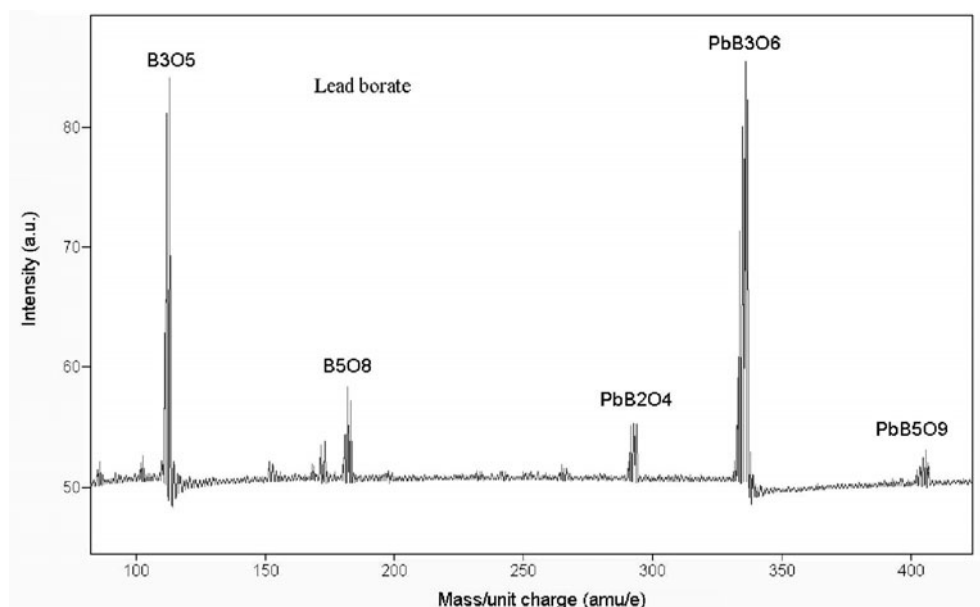


**Figure 6.** The negative-ion mass spectrum of a lead borate glass of composition  $\text{PbO}\cdot\text{B}_2\text{O}_3$ .

and appear to have no energy incentive to form stable superstructural mesounits. Generally, the height of the peak decreases as the mass increases, which we believe is due to the lesser stability of larger groups.

The LITOF-MS cannot establish the geometry of the outgoing vanadate or silicate units; we speculate that they are in the form of simple chains with varying numbers of basic units.

**3.1.2. Superstructural networks.** A second class of spectra includes those of the lead and bismuth borates and, to a great extent, the bismuth gallates. Figure 6 illustrates the negative-ion spectrum of a lead borate glass, and we note the significant decrease in the number of mass multiplets compared to the lead silicates case. Most striking is the appearance, at 336 amu, of the  $\text{PbB}_3\text{O}_6^-$  peak. Moreover, the spectrum cannot be reproduced using the ‘building block’ model, by adding a single unit multiple times, but rather some units appear more stable than others, such as  $\text{B}_3\text{O}_5^-$ ,  $\text{B}_5\text{O}_8^-$ , and  $\text{PbB}_3\text{O}_6^-$ . The spectrum also differs from that of the silicates or vanadates in that it shows no generalized decrease in the size of peaks of increasing mass, but rather displays a signature distribution of the mass multiplets.

We believe that this behaviour is due to the formation of stable superstructural units. The  $\text{PbB}_3\text{O}_6^-$  we have attributed to a boroxol or metaborate ring with a lead cation for local charge balance. Similar units appear [16] in the bismuth borate spectrum, including  $\text{BiB}_3\text{O}_6^-$ . The existence of such rings in lead borate glasses up to very high lead contents has been confirmed [13] by neutron scattering work.

In both the lead borate and silicates we also observe the formation and growth of lead oxide grouping starting at approximately 50 mol% PbO. This is to be expected: NMR work indicates [17] that the lead is in the form of  $\text{PbO}_4$  pyramids with Pb at the apex. These pyramids are believed to twist and eventually create Pb–O–Pb bonds.

The bismuth gallates are somewhat different in that they show both large molecular units and a large number of fragments, which may be the results of the variability in the

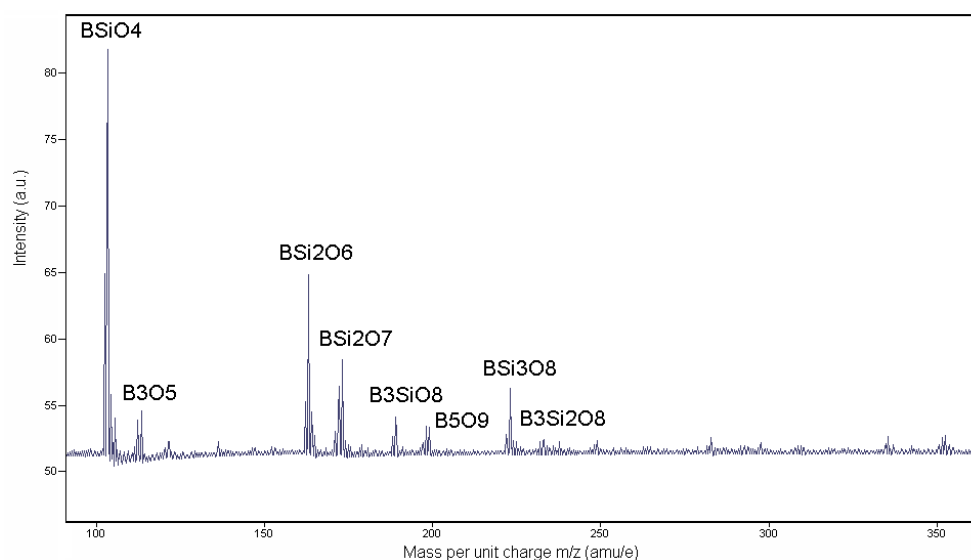


**Figure 7.** The negative-ion mass spectrum for a lead borosilicate glass of composition  $\text{PbO} \cdot \text{B}_2\text{O}_3 \cdot \text{SiO}_2$ .

coordination numbers of both bismuth and gallium. These larger mesounits are more stable in these configurations than as separate nanounits, but they are not readily attributable to discrete geometrical units.

### 3.2. Ternary glass systems

LITOF-MS can also help with other open questions. Lead borosilicate glasses are interesting from a fundamental standpoint since it is unclear to what level the borate and silicate components mix and interact. For sodium borosilicates, thermodynamics points [18] to phase separation based on the immiscibility regions at low soda contents, and thus suggests separate but co-mingled borate-rich and silicate-rich subnetworks. Wang and Stebbins [19] made  $^{17}\text{O}$  NMR measurements on sodium borosilicates, and they observed significant interactions between borate and silicate units. They noted Si–O–B (–56 ppm), Si–O–Na (–22 ppm), and B–O–Na (–22 ppm) sites, suggesting a high degree of disorder (and thus random or near-random mixing). More recent work [8] by Du and Stebbins indicates that non-ring three-coordinated borons ( $^{3}\text{B}$ ) may tend to mix with silicate groups, while  $^{31}\text{B}$  groups in rings tend to aggregate together. Martens and Muller-Warmuth [20] made NMR measurements on sodium-doped and pure borosilicates, and they agree with the mixing of borate and silicate polyhedra.

Figure 7 shows [21] a negative-ion spectrum from a lead borosilicate glass. Clearly shown are several mixed units where both boron and silicon appear in the same fragment. Indeed, we have determined mixed units to be the norm except at very low silica contents, where some ‘pure’ borate units appear. The previously noted  $\text{PbB}_3\text{O}_6^-$  unit decreases steadily once silica is added. We believe this to be the result of the immediate mixing of the silicate units with borate units, which rather quickly makes other borate units less available. This mixing has the most profound effect on mesounits that require multiple borons within the same unit, as is the case for a boroxol ring.

In the spectra we also note that lead is missing from many of the molecular groups. This suggests that the lead cation is acting as a modifier, providing charge balance, but not strongly

bound to the borosilicate network. At higher lead contents we begin to see clusters of lead and oxygen, with masses 800–1500 amu. This is not surprising, but the lack of a corresponding decrease in the few lead-containing borosilicate units points to the growth of a separate lead-oxide-rich phase within the existing network.

Finally, we observed the proposed [22] reedmergnerite unit,  $\text{BSi}_4\text{O}_{10}$ . The spectra showed small amounts of it, and we saw no evidence of fragmentation (i.e., no corresponding smaller fragments that would appear to be constituents). Thus, it does not appear to be the dominant group in the glass network.

### 3.3. Quaternary glass systems

When alkali modifiers are added to borosilicate glasses, it is natural to ask whether the doping cations prefer to go [17] to sites that are ‘borate-like’, ‘silicate-like’, or whether there is no preference. Different sites are believed to exist in some borate glasses, as indicated by the work of Kamitsos and Duffy [23, 24]. Avoidance [25, 26] has also been noted in other glass systems. The LITOF-MS data can provide [21] a preliminary answer to this structural question, in the sample cases of the  $0.33\text{Na}_2\text{O}\cdot 0.3\text{PbO}\cdot \text{B}_2\text{O}_3\cdot \text{SiO}_2$  and  $1.05\text{Na}_2\text{O}\cdot 1.3\text{PbO}\cdot \text{B}_2\text{O}_3\cdot \text{SiO}_2$ . For simplicity, we use the designation  $Y$  to refer to the ratio of soda to bora, namely 0.33 or 1.05.

Early work on the role of modifier cations in borosilicates was done by Bray *et al* [22, 27]. In their borosilicate glasses doped with sodium, the cations were believed to show an initial preference for borate sites, only occupying silicate sites when the amount of alkali metal exceeded a threshold that depended on the relative amount of silica in the glass.

The LITOF-MS provides some insights into this issue of cation preference. We do note that our glasses differ in stoichiometry from those of the previous researchers, as they contain lead oxide. Both of our glass compositions show strong B–Si mixing, in the form of units such as  $\text{BSiO}_4$ ,  $\text{BSi}_2\text{O}_6$ ,  $\text{B}_3\text{SiO}_7$ , and  $\text{B}_3\text{SiO}_8$ . The sodium ions only associate with borate units for the  $Y = 0.33$  sample (see figure 8), but are shared with some borosilicate units for the  $Y = 1.05$  glass. The borate association remains dominant, however, even as we increase the soda content. We thus believe that sodium cations prefer the borate sites early on, further evidenced by the fact that all the clusters can be attained by substituting  $(\text{BO})^+$  for  $\text{Na}^+$ . These observations are in agreement with the work of Dell and Bray, Wang and Stebbins, and Martens and Muller-Warmuth.

The TOF spectra of these quaternary glasses also show the reedmergnerite unit, but only in small quantities. We see no evidence of diborates, which are argued against by the NMR work [19].

## 4. Conclusions

We have reported on a variety of applications of LITOF-MS to glass systems. The technique provided new insights as well as confirmation of multiple NMR results. In summary, the instrument was able to: distinguish highly fragmented from superstructural networks; measure a  $(\text{PbB}_3\text{O}_6)^-$  units attributed to a boroxol or metaborate ring; look at the mixing of boron and silicon in borosilicate mesounits; determine borate site preferences for sodium ions entering lead borosilicate networks; and measure the reedmergnerite unit at low abundance.

## Acknowledgments

We would like to acknowledge the financial support of the National Science Foundation under grant DMR-PECASE 9733724. The authors would also like to thank Coe College for its

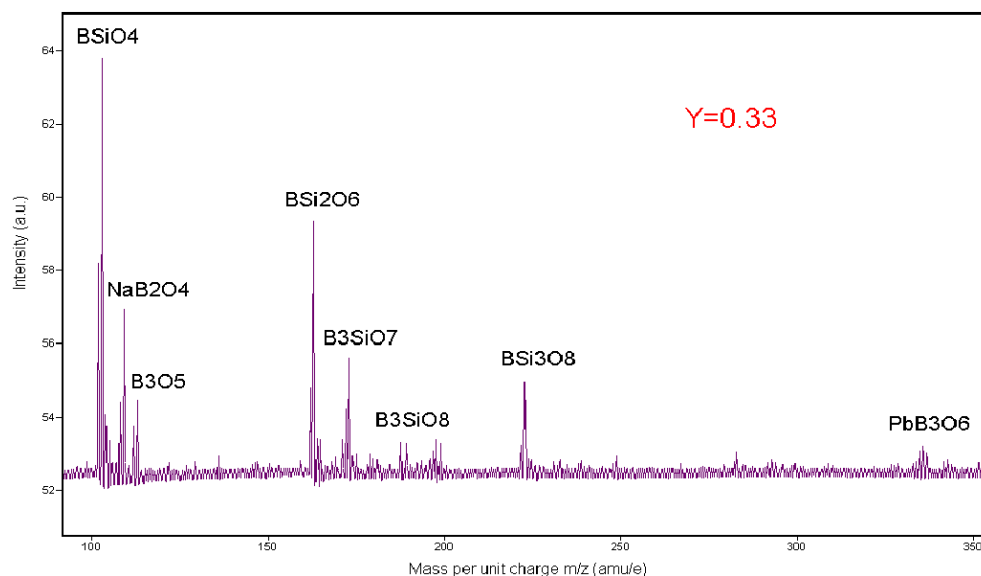


**Figure 8.** The negative-ion mass spectrum for the sodium-doped lead borosilicate glass of composition  $0.33\text{Na}_2\text{O}\cdot 0.3\text{PbO}\cdot \text{B}_2\text{O}_3\cdot \text{SiO}_2$ .

unwavering help, and the organizers of the special symposium held at the Fall meeting of the Glass and Optical Materials Division of the American Ceramic Society in Pittsburgh, PA.

## References

- [1] Meera B N and Ramakrishna J 1993 *J. Non-Cryst. Solids* **159** 1
- [2] Kreidl N J 1983 *Inorganic Glass Forming Systems* (New York: Academic) ch 3
- [3] Wright A C, Vedishcheva N M and Shakhmatkin B A 1997 *What Can Crystallography Tell Us About the Intermediate Range Order in Borate Glasses?* (New York: Plenum)
- [4] Hoppe U, Kranold R, Weber H J, Neufeind J and Hannon A C 2000 *J. Non-Cryst. Solids* **278** 99
- [5] Joo C, Werner-Zwanziger U and Zwanziger J W 2000 *J. Non-Cryst. Solids* **261** 282
- [6] Youngman R E, Werner-Zwanziger U and Zwanziger J W 1996 *Z. Naturf. a* **51** 321
- [7] Ratai E M, Janssen M, Epping J D, Chan J C C and Eckert H 2002 Local and medium range order in alkali borate glasses: an overview of recent solid state NMR results *4th Int. Conf. on Borate Glasses, Crystals and Melts (Cedar Rapids, IA, 2002)* ed A C Wright, S Feller, N M Vedishcheva and M Affatigato (Sheffield: Society of Glass Technology)
- [8] Du L S and Stebbins J 2003 *J. Non-Cryst. Solids* **315** 239
- [9] Wright A C 1993 *Neutron and X-ray Amorphography* (Westerville, OH: American Ceramic Society)
- [10] Sinclair R, Stone C E, Wright A C, Polyakova I G, Vedishcheva N M, Shakhmatkin B A, Feller S, Johanson B C, Venhuizen P, Williams R B and Hannon A C 2000 *Phys. Chem. Glasses* **41** 286
- [11] Haglund R F 1998 *Mechanisms of Laser-Induced Desorption and Ablation* (San Diego, CA: Academic)
- [12] Duffy J A and Ingram M D 1991 *Optical Basicity* (Westerville: American Ceramic Society)
- [13] Bach H and Duffy J A 1981 *Phys. Chem. Glasses* **22** 86
- [14] Duffy J A and Kyd G O 1995 *Phys. Chem. Glasses* **36** 101
- [15] Stentz D, Blair S, Goater C, Feller S and Affatigato M 2000 *Appl. Phys. Lett.* **76** 1
- [16] Stentz D, Blair S, Goater C, Feller S and Affatigato M 2000 *Phys. Chem. Glasses* **41** 259
- [17] Varshneya A 1994 *Fundamentals of Inorganic Glasses* (San Diego, CA: Academic)
- [18] Shelby J E 1997 *Introduction to Glass Science and Technology* (Cambridge: Royal Society of Chemistry)
- [19] Wang S and Stebbins J 1999 *J. Am. Ceram. Soc.* **82** 1519
- [20] Martens R and Muller-Warmuth W 2000 *J. Non-Cryst. Solids* **265** 167
- [21] Blair S, Stentz D, Goater C, Feller S and Affatigato M 2001 *J. Non-Cryst. Solids* **293–295** 416

- 
- [22] Dell W J, Bray P J and Xiao S Z 1983 *J. Non-Cryst. Solids* **58** 1
- [23] Duffy J A, Harris B, Kamitsos E I, Chryssikos G D and Yiannopoulos Y D 1997 *J. Phys. Chem. B* **101** 4188
- [24] Kamitsos E I and Chryssikos G D 1998 *Solid State Ion.* **105** 75
- [25] Shelby J E 1975 *J. Appl. Phys.* **46** 193
- [26] Lee S K and Stebbins J 1999 *Am. Mineral.* **84** 937
- [27] Kim K S, Bray P J and Merrin S 1976 *J. Chem. Phys.* **64** 4459